Hindawi Publishing Corporation
Shock and Vibration
Volume 2015, Article ID 624712, 8 pages
http://dx.doi.org/10.1155/2015/624712

Research Article

Investigation of Equivalent Unsprung Mass and Nonlinear Features of Electromagnetic Actuated Active Suspension

Jun Yin,[1] Xinbo Chen,[1,2] Jianqin Li,[1] and Lixin Wu[1]

[1]*Clean Energy Automotive Engineering Center, Tongji University, Shanghai 201804, China*
[2]*School of Automotive Studies, Tongji University, Shanghai 201804, China*

Correspondence should be addressed to Xinbo Chen; austin_1@163.com

Received 5 May 2015; Revised 4 August 2015; Accepted 9 August 2015

Academic Editor: Rafał Burdzik

Electromagnetic actuated active suspension benefits active control and energy harvesting from vibration at the same time. However, the rotary type electromagnetic actuated active suspension introduces a significant extra mass on the unsprung mass due to the inertia of the rotating components of the actuator. The magnitude of the introduced unsprung mass is studied based on a gearbox type actuator and a ball screw type actuator. The geometry of the suspension and the actuator also influence the equivalent unsprung mass significantly. The suspension performance simulation or control logic derived should take this equivalent unsprung mass into account. Besides, an extra force should be compensated due to the nonlinear features of the suspension structure and it is studied. The active force of the actuator should compensate this extra force. The discovery of this paper provides a fundamental for evaluating the rotary type electromagnetic actuated active suspension performance and control strategy derived as well as controlling the electromagnetic actuated active suspension more precisely.

1. Introduction

Suspension is the critical component to isolate vibration excited by uneven road and to ensure driving safety of a vehicle. The passive suspension is widely used for its sufficient performance and relative low cost. However, due to the fixed parameters of the spring stiffness and the damper coefficient, the passive suspension can only reach an acceptable compromise between ride comfort and road holding. Active suspension is an appropriate alternative for its adjustable control force according to different conditions. However, in consideration of fuel economy and environmental friendliness, large energy consumed by conventional active suspension is not acceptable. The clean energy automobile (such as pure electric vehicle, hybrid vehicle, and fuel cell vehicle) is equipped with a high voltage battery normally and thus provides an energy storage system. There is a chance to develop the electromagnetic actuated active suspension which can control the suspension and realize energy harvesting from vibration at the same time.

A lot of research interests of the electromagnetic active suspension have arisen. The electromagnetic actuator is based on either linear electromagnetic motors or rotary electromagnetic motors. Bose Company, Gysen et al., and Suda et al. researched and developed linear electromagnetic motors to improve vehicle dynamics while consuming less energy [1–5]. Based on rotary electromagnetic motor, Zheng et al. proposed an electromagnetic actuator which includes a brushless DC motor and a ball screw [6]. Yin et al. utilize conventional permanent magnet synchronous motor (PMSM) and design proper mechanism to realize electromagnetic actuated active suspension [7]. Zuo and Zhang researched in both linear and rotary approaches for electromagnetic actuator design [8, 9]. The linear type normally increases the sprung and unsprung mass in an ignorable magnitude. However, the inertia of the rotating components of the rotary type would act like a significant extra mass especially on the unsprung mass. Besides, to maintain a constant relative speed between the sprung mass and the unsprung mass, an extra force should be applied due to the nonlinear features of a given suspension structure.

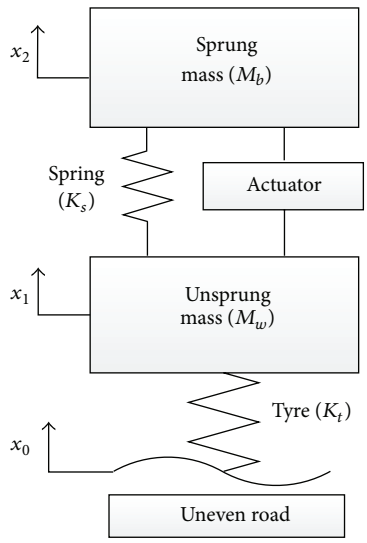

Figure 1: Quarter car model of active suspension.

These issues would influence the suspension dynamic model; thus the control logic derived might lead to an incorrect situation.

To figure out the introduced unsprung mass caused by the inertia of the rotating components, this paper takes a gearbox type and a ball screw type electromagnetic actuated active suspension for example, and it proposed the so-called equivalent unsprung mass and analyzed the magnitude. Based on the suspension structure proposed by Chen and Zhao the extra force caused by the nonlinear features of the suspension structure is analyzed.

To show the importance of an accurate unsprung mass, Section 2 presents a quarter car model of conventional active suspension and its dynamic equations. Equivalent unsprung masses of gearbox type and ball screw type actuators are analyzed and discussed in Section 3. In Section 4, the extra force caused by the nonlinear features of the given suspension structure will be discussed and conclusions are drawn in Section 5.

2. Quarter Car Model

A quarter car model is usually utilized to simply analyze the ride comfort and road holding of the suspension. And the half car model and full car model can be derived accordingly. Figure 1 shows a widely used quarter car model of active suspension, which is modeled as a two-degree-of-freedom system, which includes the sprung mass M_b, the unsprung mass M_w, the spring stiffness K_s, the tyre stiffness K_t, and the force of the actuator U.

The displacement of the sprung mass, unsprung mass, and road input are denoted as x_2, x_1, and x_0. The dynamic equations of the quarter car model can be expressed as

$$\begin{aligned} M_b\ddot{x}_2 &= K_s\left(x_1 - x_2\right) + U, \\ M_w\ddot{x}_1 &= K_s\left(x_2 - x_1\right) + K_t\left(x_0 - x_1\right) - U. \end{aligned} \tag{1}$$

Normally, the parameter of the unsprung mass is a constant which only includes the conventional components such as the tyre, rim, knuckle, brake disc, and calipers. However, the inertia of the actuator rotating components contributes the unsprung mass actually. Given the force to the unsprung mass, not only would the unsprung mass react with an acceleration, but also the rotating components would react with an angular acceleration. Therefore, the actual unsprung mass would be no longer a constant. Based on the research, the equivalent unsprung mass is defined as the additional unsprung mass introduced by the actuator. Examples of equivalent unsprung mass are given in Section 3. Moreover, the active force which is derived from normal quarter car model and control logic should compensate the extra force which is caused by the nonlinear features of a given suspension structure. Therefore the dynamic equations of the quarter car model given above would be no longer accurate in real applications.

3. Equivalent Unsprung Mass of Actuator

As discussed above, the mass or the inertia of the actuator rotating components would introduce an extra unsprung mass. Thus the simulation of the suspension performance and active force derived by normal quarter car model would not be appropriate. To show the magnitude of the introduced unsprung mass, calculations are carried out by a gearbox type and a ball screw type electromagnetic actuated active suspension. To simplify the study, the spring is neglected and a fixed displacement of sprung mass is assumed first; then the combined dynamic effect of sprung mass and unsprung mass is discussed.

3.1. Gearbox Type. Based on double wishbone suspension, Yin et al. proposed an active and energy regenerative suspension structure which is shown in Figure 2 and its actuator is shown in Figure 3. The actuator is fixed on the sprung mass. Structure overview and actuator design are detailed in [7].

The relative displacement of the sprung mass and the unsprung mass is assumed to be −80 mm~+80 mm for conventional applications. Assuming a displacement fixed sprung mass, when the unsprung mass bumps up and down, the unsprung mass speed represents the relative speed between the sprung mass and the unsprung mass. It is obvious that a specific bell crank rotation speed is corresponding to this unsprung mass speed. The relationship of the bell crank rotation speed and the unsprung mass speed can be described as

$$\omega_b = i_{\text{stru}}(h) \cdot v_{\text{un}}, \tag{2}$$

where h denotes the relative position between the sprung mass and the unsprung mass, ω_b is the bell crank rotation speed, $i_{\text{stru}}(h)$ is the transmission ratio of the bell crank rotation speed and the unsprung mass speed which is determined by the given structure, and v_{un} is the unsprung mass speed.

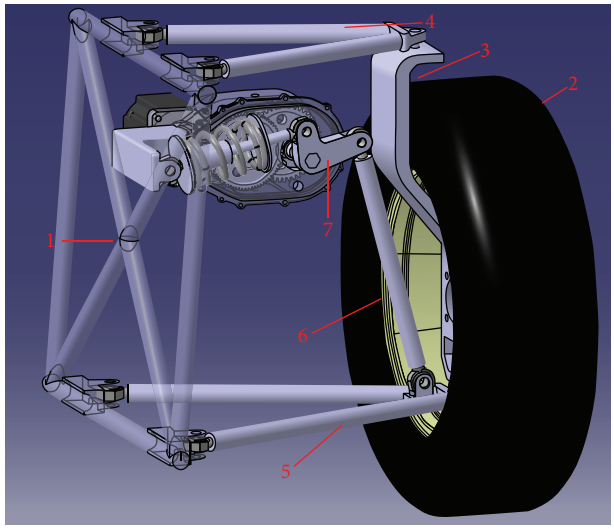

Figure 2: Gearbox type active suspension structure. (1) Frame; (2) wheel; (3) knuckle; (4) upper A-arm; (5) lower A-arm; (6) push bar; (7) actuator.

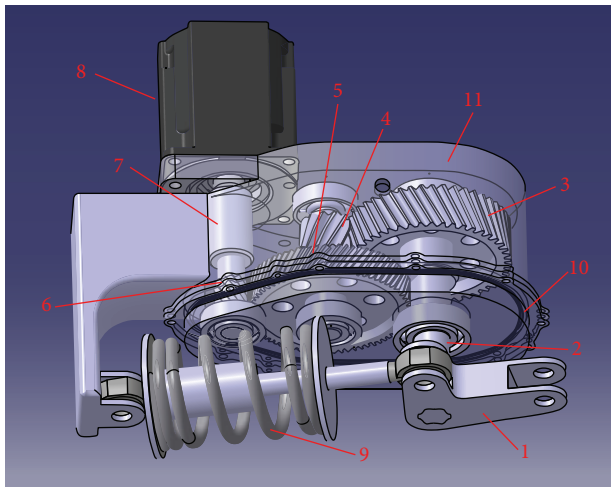

Figure 3: Gearbox type actuator. (1) Bell crank; (2) output shaft; (3) second-stage driven gear; (4) second-stage driving gear; (5) first-stage driven gear; (6) first-stage driving gear; (7) input shaft; (8) PMSM; (9) spring; (10) Shell 1; (11) Shell 2.

Since the bell crank angular acceleration and the unsprung mass acceleration are derivatives of bell crank rotation angular speed and unsprung mass speed, respectively, a similar relationship can be obtained:

$$\alpha_b = i_{\text{stru}}(h) \cdot a_{\text{un}}, \tag{3}$$

where α_b is the bell crank angular acceleration and a_{un} is the unsprung mass acceleration.

From the view of the actuator, the motor torque is increased and the motor rotation speed is decreased through a dual stage gearbox. The parameters of the gearbox are shown in Table 1.

Table 1: Gearbox parameters.

	Inertia (kg·cm^2)	Teeth
Motor shaft	9.12	\
1st-stage driving gear	6.394	14
1st-stage driven gear	30	71
2nd-stage driving gear & middle shaft	6.057	13
2nd-stage driven gear	50	46
Output shaft	1.348	\

Given the bell crank rotation speed ω_b, the motor rotation speed is determined by

$$\omega_m = i_g \cdot \omega_b, \tag{4}$$

where ω_m is the motor rotation speed and i_g is the gear ratio and it equals 17.95.

To evaluate the equivalent unsprung mass introduced by the inertia of the motor shaft, gears, and gear shafts, an equivalent inertia of the output shaft is calculated first. Take the motor shaft, for example,

$$\begin{aligned} T_m &= J_m \cdot \alpha_m, \\ \alpha_o &= i_g \cdot \alpha_m, \\ T_o &= i_g \cdot T_m, \\ T_o &= J_{\text{meq}} \cdot \alpha_o, \end{aligned} \tag{5}$$

where T_m, J_m, α_m, T_o, α_o, and J_{meq} represent motor torque, inertia of motor shaft, motor shaft angular acceleration, output shaft torque, output shaft angular acceleration, and equivalent inertia of motor shaft, respectively.

From (5), J_{meq} can be calculated as

$$J_{\text{meq}} = i_g^2 \cdot J_m. \tag{6}$$

Thus a total equivalent inertia of the output shaft can be obtained, and it is 0.55 kg·m^2.

Applying a force to the unsprung mass, both the unsprung mass and rotation components would react with an acceleration. Fixing the sprung mass and keeping a constant relative acceleration of 1 m/s^2 of the unsprung mass, the force applied varies because the influence of the equivalent inertia of output shaft is different corresponding to different relative position between the sprung mass and the unsprung mass. (Equation (3) reveals a transmission ratio between the acceleration of the unsprung mass and the angular acceleration of the actuator.) This equivalent inertia of output shaft can be thus equaled to an equivalent unsprung mass in wheel side corresponding to different relative position between the sprung mass and the unsprung mass. The magnitude of the equivalent unsprung mass is equaled to the applied force since the relative acceleration is 1 m/s^2. The calculation of

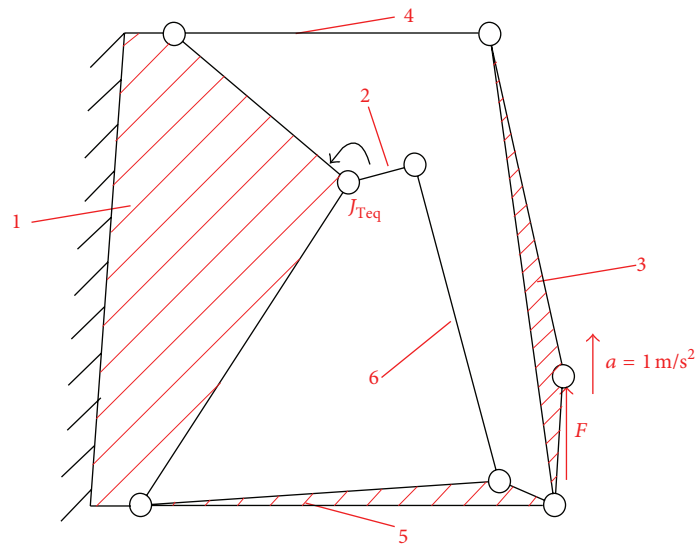

Figure 4: Planar view of suspension structure. (1) Frame; (2) bell crank; (3) knuckle; (4) upper A-arm; (5) lower A-arm; (6) push bar; (7) actuator.

the equivalent unsprung mass is done by a simulation in ADAMS.

In this simulation, the freedom of steering is fixed. The suspension structure shown in Figure 2 is simplified as a planar mechanism with 1 DOF and it is shown in Figure 4. The inertia or mass of any other component is set to be 0 except the total equivalent inertia of the output shaft which is represented by J_{meq} shown in Figure 4.

In relative position of the unsprung mass and the sprung mass from −80 mm to 80 mm, with a 0 m/s relative speed of the unsprung mass and the sprung mass and a 1 m/s^2 relative acceleration of the unsprung mass and the sprung mass, the equivalent unsprung mass is shown in Figure 5.

Figure 5 shows a significant unsprung mass introduced by the equivalent inertia of output shaft, and it is also influenced by the geometry of the suspension and the actuator significantly especially closing to the relative position limit of the unsprung mass and the sprung mass. The equivalent unsprung mass varies from 109.8 kg to 49.3 kg corresponding to different relative position between the sprung mass and the unsprung mass.

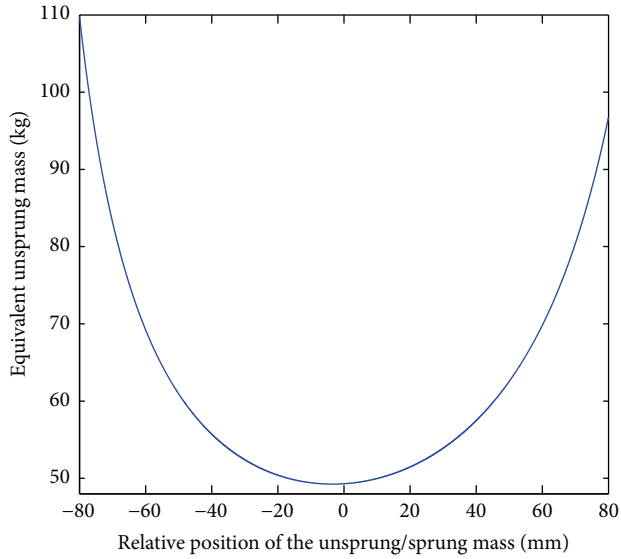

Figure 5: Equivalent unsprung mass versus different relative position of the unsprung mass.

3.2. Ball Screw Type. Yu, Zheng, and Zhang et al. realized the actuator of the active suspension by utilizing a permanent magnet brushless DC motor with a ball screw [10, 11]. The assembly of the actuator is shown in Figure 6 and the section view is shown in Figure 7 [12].

In this configuration, the screw is connected with the link of the suspension which becomes part of the unsprung mass. The nut of the screw is connected with the rotor of the motor. The stator and the shell of the motor are connected with the sprung mass. Given a relative speed between the sprung mass and the unsprung mass, a corresponding rotation speed of the nut and the motor shaft is expected. A similar planar view of the active suspension structure utilizing ball screw mechanism is shown in Figure 8. The push bar of the gearbox type is replaced by a motor, a nut, and a screw.

Fixing the sprung mass and keeping a constant relative acceleration of 1 m/s^2 of the unsprung mass, a force is needed to accelerate the nut and the motor shaft. To simplify the calculation of the equivalent unsprung mass introduced by the ball screw mechanism, the influence of the suspension mechanism is neglected and the displacement of the nut is assumed as a strict proportion of the unsprung mass:

$$s_1 = \frac{L1}{L2} \cdot s,$$
$$a_1 = \frac{L1}{L2} \cdot a, \tag{7}$$

Figure 6: Ball screw type actuator.

Table 2: Parameters of ball screw type suspension.

Angular displacement of 1 round (n_0)	2π
Lead of the screw (P_h)	30 mm
Efficiency of the driving mode (η_d)	0.995
Efficiency of the braking mode (η_b)	0.992
Inertia of motor shaft (J_m)	9.12 kg·cm^2
Inertia of nut (J_n)	0.9 kg·cm^2

where s, s_1, a, and a_1 are displacement of unsprung mass, acceleration of unsprung mass, relative displacement between the nut and the screw, and relative acceleration between the nut and the screw. Consider $L1/L2 = 0.85$.

For a ball screw mechanism, 1 round rotation of the nut results in a relative displacement which equals the lead of the ball screw. Thus an angular displacement of the nut is a proportion of the relative displacement of the nut and the screw. Since the screw is connected with the lower arm via a revolute joint, the screw cannot be rotated along its axis. The angular acceleration of the nut is thus a proportion of the relative acceleration of the nut and the screw. Consider

$$\begin{aligned} s_1 &= \int_{t_0}^{t_1} a_1 t \, dt, \\ n &= \int_{t_0}^{t_1} \alpha t \, dt, \end{aligned} \tag{8}$$

where n is the angular displacement and α is the angular acceleration.

Combining (7) and (8),

$$\alpha = a_1 \cdot \frac{n}{s_1} = a \cdot \frac{n}{s} = a \cdot \frac{n_0}{P_h}, \tag{9}$$

where n_0 is the angular displacement of 1 round. P_h is the lead of the screw.

When rotation motion is converted into linear motion, the ball screw mechanism is working in the driving mode. When linear motion is converted into rotation, the ball screw mechanism is working in the braking mode. The relationship between the torque of the nut and the axis force of the screw can be described as follows:

$$\begin{aligned} T_d &= \left(J_m + J_n\right) \cdot \alpha = \frac{F \cdot L2/L1 \cdot P_h}{2\pi \cdot \eta_d}, \\ T_b &= \left(J_m + J_n\right) \cdot \alpha = \frac{F \cdot L2/L1 \cdot P_h \cdot \eta_b}{2\pi}, \end{aligned} \tag{10}$$

where T_d is the driving torque of the nut, F is force in wheel side, η_d is the efficiency of the driving mode, η_b is the efficiency of the braking mode, J_m is the inertia of motor shaft, and J_n is the inertia of nut.

Parameters of ball screw type suspension are given in Table 2.

Similar to the gearbox type active suspension, fixing the sprung mass and keeping a constant relative acceleration of 1 m/s^2 of the unsprung mass, an axis force of the screw should be applied to accelerate the inertia of the motor shaft and the nut. This axis force of the screw should be balanced with the force in wheel side. This force in wheel side can be equaled to an equivalent unsprung mass in wheel side. The value of the equivalent unsprung mass is equaled to the force applied in wheel side since the relative acceleration is 1 m/s^2.

Combining (9) and (10), the equivalent unsprung mass is 37.2 kg in driving mode and 37.7 kg in braking mode. Moreover, taking the geometry of the suspension into account, the equivalent unsprung mass of the ball screw type would vary in the same way with the gearbox type discussed before.

3.3. Discussion. The simulation of gearbox type active suspension and the calculation of ball screw type active suspension show significant unsprung masses introduced by the rotating components of the actuators. And this introduced unsprung mass is also influenced by the geometry of the suspension significantly.

However, the simulation and calculation above are based on the assumption of a displacement fixed sprung mass. In real situation, the displacement of the sprung mass is not fixed and thus the force to accelerate or decelerate the rotating components is relevant to the acceleration or deceleration of both the sprung mass and the unsprung mass. Figuring out that the equivalent unsprung mass ($M_{\text{eq}}(h)$) corresponds to different relative position between the sprung mass and the unsprung mass, a lookup table of $M_{\text{eq}}(h)$ can be made. In the quarter car suspension performance simulation, an additional mass (M_{ad}) can be added to the unsprung mass. And this additional mass (M_{ad}) can be calculated by

$$M_{\text{ad}} = M_{\text{eq}}(h) \cdot \frac{a_w - a_b}{a_w}, \tag{11}$$

where a_b is the acceleration of the sprung mass and a_w is the acceleration of the unsprung mass.

It should be noted that the equivalent unsprung mass is calculated based on the assumption of a 0 m/s relative speed and a 1 m/s^2 relative acceleration between the sprung mass and the unsprung mass. The additional mass M_{ad} added to the quarter car model would vary corresponding to different relative position between the sprung mass and the unsprung mass and different relative acceleration of the unsprung mass

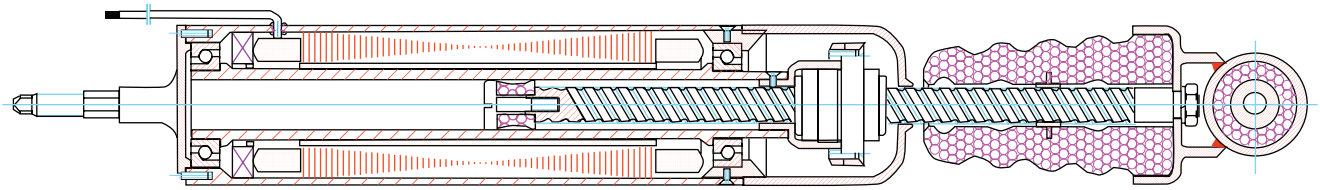

Figure 7: Section view of the ball screw type actuator.

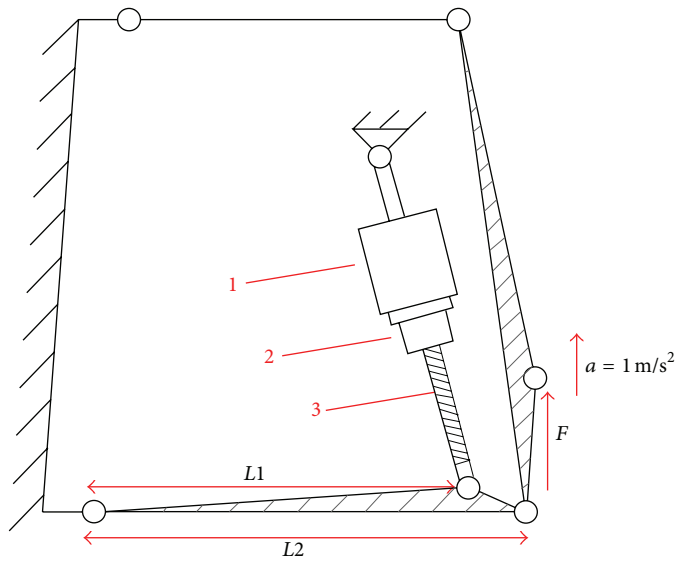

Figure 8: Ball screw type suspension structure. (1) Motor; (2) nut; (3) screw.

and the sprung mass. It is not related with the relative speed between the sprung mass and the unsprung mass.

4. Influence of Suspension Kinetics Characteristic

Research shows the equivalent damping and stiffness of the suspension exhibit obvious nonlinear features of spatial structure [13–15]. However, the nonlinear features of the suspension structure also influence the kinetics of the unsprung mass.

Take the gearbox type active suspension for example. Assuming a 1 m/s relative speed between the sprung mass and the unsprung mass, in relative position of the unsprung mass and the sprung mass from −80 mm to 80 mm, the rotation speeds of the motor shaft are shown in Figure 9.

From Figure 9 we can figure out that, to maintain a constant relative speed between the sprung mass and the unsprung mass, a force should be applied to accelerate or decelerate the motor shaft, as well as the other rotating components of the actuator. The magnitude of the force applied in the wheel side corresponds to different relative position and different relative speed between the sprung mass and the unsprung mass. To maintain a 1 m/s relative speed between the sprung mass and the unsprung mass in relative position of the unsprung mass and the sprung mass from −80 mm to 80 mm, the magnitude of the force applied in wheel side is shown in Figure 10.

Varying different relative speed between the sprung mass and the unsprung mass, the force applied in the wheel side can be derived from the equation shown below and the proof is omitted:

$$F_{\mathrm{comp}}(h)\big|_{v=v_i} = \left(\frac{v_i}{v_0}\right)^2 F_{\mathrm{comp}}(h)\Big|_{v=v_0}, \tag{12}$$

where v_0, v_i, $F_{\mathrm{comp}}(h)|_{v=v_0}$, and $F_{\mathrm{comp}}(h)|_{v=v_i}$ represent 1 m/s relative speed between the sprung mass and the unsprung mass, current relative speed between the sprung mass and the unsprung mass, the extra force that needs to be compensated in relative speed v_0, and the extra force that needs to be compensated in current relative speed, respectively.

It should be noted that the extra force that needs to be compensated is calculated based on the assumption of a 1 m/s relative speed and a $0\,\mathrm{m/s^2}$ relative acceleration between the sprung mass and the unsprung mass. The extra force that needs to be compensated in current relative speed $F_{\mathrm{comp}}(h)|_{v=v_i}$ would vary corresponding to different relative position between the sprung mass and the unsprung mass and different relative speed of the unsprung mass and

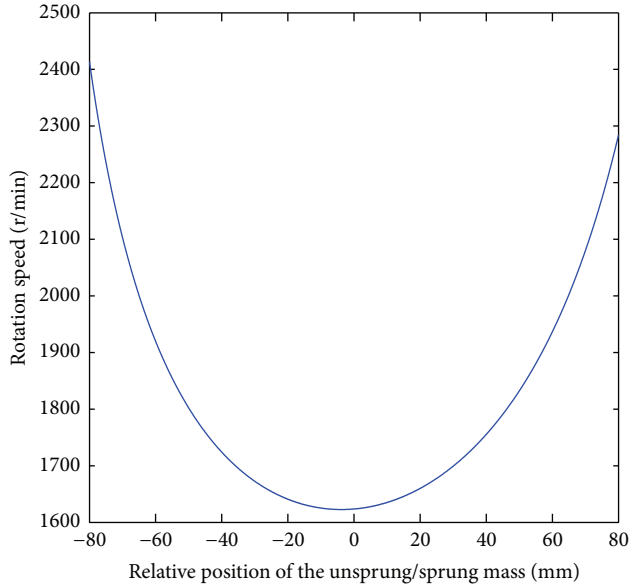

Figure 9: Rotation speeds of the motor shaft versus different relative position of the unsprung mass.

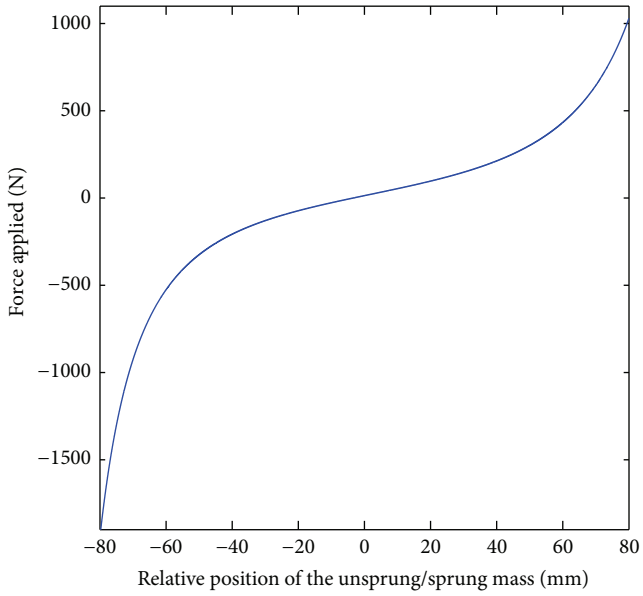

Figure 10: Force applied in wheel side versus different relative position of the unsprung mass.

the sprung mass. It is not related with the relative acceleration between the sprung mass and the unsprung mass.

5. Conclusion

The rotating components of the electromagnetic active suspension actuator would introduce a significant equivalent unsprung mass. This may lead to an inaccurate result of the quarter car suspension performance simulation since the unsprung mass is a constant in such simulations, and the control logic derived may not suit the real situation well. The magnitude of the equivalent unsprung mass is studied by two application examples. The geometry of the suspension structure also influences the equivalent unsprung mass significantly and it is studied. To maintain a constant relative speed between the sprung mass and the unsprung mass, an extra force should be applied corresponding to different relative position and different relative speed between the sprung mass and the unsprung mass.

In practice, the equivalent unsprung mass of a determined electromagnetic active suspension actuator can be studied first and stored as a lookup table. The extra force that needs to be compensated which is introduced by the geometry of the suspension structure can be studied first and stored as another lookup table. These lookup tables are then utilized in the simulation and controller, respectively. The simulation or control logic derived should take this equivalent unsprung mass into account. And the active force of the actuator should compensate the extra force introduced by the geometry of the suspension structure. Thus the simulation or control logic derived meets the real situation and the ideal active force can be realized in real controlling.

This research is based on two examples of the rotating type electromagnetic actuated active suspension. However, the discovery of this paper provides a fundamental for evaluating the rotary type electromagnetic actuated active suspension performance and control strategy derived as well as controlling the active suspension more precisely.

Conflict of Interests

The authors declare that there is no conflict of interests regarding the publication of this paper.

Acknowledgment

This project is partially supported by the National Nature Science Foundation of China (51375344). The authors would like to express their sincere thanks to the foundation for providing research funding.

References

[1] W. D. Jones, "Easy ride: Bose Corp. uses speaker technology to give cars adaptive suspension," *IEEE Spectrum*, vol. 42, no. 5, pp. 12–14, 2005.

[2] B. L. J. Gysen, J. J. H. Paulides, J. L. G. Janssen, and E. A. Lomonova, "Active electromagnetic suspension system for improved vehicle dynamics," *IEEE Transactions on Vehicular Technology*, vol. 59, no. 3, pp. 1156–1163, 2010.

[3] B. L. J. Gysen, J. L. G. Janssen, J. J. H. Paulides, and E. A. Lomonova, "Design aspects of an active electromagnetic suspension system for automotive applications," *IEEE Transactions on Industry Applications*, vol. 45, no. 5, pp. 1589–1597, 2009.

[4] B. L. J. Gysen, T. P. J. van der Sande, J. J. H. Paulides, and E. A. Lomonova, "Efficiency of a regenerative direct-drive electromagnetic active suspension," *IEEE Transactions on Vehicular Technology*, vol. 60, no. 4, pp. 1384–1393, 2011.

[5] Y. Suda, S. Nakadai, and K. Nakano, "Hybrid suspension system with skyhook control and energy regeneration (development of

self-powered active suspension)," *Vehicle System Dynamics*, vol. 29, supplement 1, pp. 619–634, 1998.

[6] X.-C. Zheng, F. Yu, and Y.-C. Zhang, "Novel energy-regenerative active suspension for vehicles," *Journal of Shanghai Jiaotong University*, vol. 13, no. 2, pp. 184–188, 2008.

[7] J. Yin, X. B. Chen, and J. Q. Li, "Design and analysis of an active and energy regenerative suspension," in *Proceedings of the 2015 IFToMM World Congress*, October 2015.

[8] L. Zuo and P.-S. Zhang, "Energy harvesting, ride comfort, and road handling of regenerative vehicle suspensions," *Journal of Vibration and Acoustics*, vol. 135, no. 1, Article ID 011002, 2013.

[9] P. S. Zhang, *Design of electromagnetic shock absorbers for energy harvesting from vehicle suspensions [M.S. thesis]*, Stony Brook University, Stony Brook, NY, USA, 2010.

[10] X. C. Zheng, *Theoretical and experimental study of automobile electrical energy-regenerative active suspension [M.S. thesis]*, Shanghai Jiao Tong University, Shanghai, China, 2007.

[11] Y. C. Zhang, X. C. Zheng, F. Yu et al., "Theoretical and experimental study on electrical energy-regenerative suspension," *Automotive Engineering*, vol. 30, no. 1, pp. 48–52, 2008.

[12] Y. C. Zhang, *Study on robust control for vehicle active electromagnetic suspension [Ph.D. thesis]*, Shanghai Jiao Tong University, Shanghai, China, 2012.

[13] G. B. Ning, L. G. Zhang, Z. P. Yu, and X. B. Chen, "Modelling and analysis of the nonlinear characteristics of spatial structurure in double wishbone suspension with torsion bar," *Automotive Engineering*, vol. 32, no. 2, pp. 143–147, 2010.

[14] X. B. Chen and R. Zhao, "Nonlinear analysis and design of double wishbone suspension with torsion," *Journal of Tongji University*, vol. 34, no. 5, pp. 655–659, 2006.

[15] X. Y. Li, Y. Zhang, L. S. Zhou, and M. Peng, "Characteristic analysis and calculation of wishbone independent suspension with torsion bar," *Automotive Engineering*, vol. 25, no. 1, pp. 15–20, 2003.